Estimating long-term microclimatic conditions for long-range sound propagation studies

Yves Brunet, Jean-Pierre Lagouarde, Vadim Zouboff

7th Long Range Sound Propagation Symposium
Ecole Centrale de Lyon, France, 24-26 July 1996

Estimating long-term microclimatic conditions for long-range sound propagation studies

Y. BRUNET [1], J.P. LAGOUARDE [1] and V. ZOUBOFF [2]

[1] *INRA-Bioclimatologie, BP 81, 33883 Villenave d'Ornon cedex (France)*

[2] *Laboratoire Régional des Ponts et Chaussées d'Angers, BP 69, 49136 Les Ponts de Cé cedex (France)*

ABSTRACT

Sound propagation in the lower atmosphere strongly depends on the wind direction and the vertical gradients in the speed of sound. The latter depends in turn on the vertical gradients of wind velocity and temperature. Because of the natural space and time fluctuations in microclimatic conditions, the acoustic level at a large distance from the source must be considered as a random variable. Therefore, knowing the statistical characteristics of the fluctuations in microclimatic conditions is of great importance for estimating the accuracy of a measurement or a calculation of long-range acoustic levels.

We describe a method based on a heat and mass transfer simulation model, for estimating hourly variations in local wind and temperature profiles. Two types of inputs are required:

- site descriptors (soil and vegetation parameters acting on the surface energy and water balances: albedo, roughness length, soil type...);
- standard climatic data provided by the meteorological network (insolation, wind velocity and direction, air temperature and humidity, precipitation...).

Using long-term (i.e., several years) climatic data files, it is possible to calculate statistical distributions of the vertical wind and temperature gradients at some height above the surface, as well as the distribution of the vertical sound velocity gradient. For a given source-receiver configuration, the corresponding distribution function of sound levels can then be deduced.

The method is illustrated by a case study perfomed with a 30 year climatic file for a typical rural site in France. As an example, we calculated the fraction of time during which the sound level exceeded a prescribed threshold, for one particular source-receiver configuration.

1. INTRODUCTION

Knowledge of the statistical properties of the sound pressure level is very important from a practical point of view. Sound propagation in the lower atmosphere strongly depends on the wind direction and the vertical gradients in the speed of sound. The latter depends in turn on the vertical gradients of wind velocity and temperature. Because of the natural space and time fluctuations in microclimatic conditions, the acoustic level at a large distance from

the source must be considered as a random variable. Therefore, knowing the statistical characteristics of the fluctuations in microclimatic conditions on a given site is of great importance for estimating the accuracy of a measurement or a calculation of long-range acoustic levels.

The vertical gradients in horizontal wind velocity and air temperature cannot be determined on the sole basis of the climatic data given by meteorological networks. Temperature gradients (and wind speed gradients, through the influence of stability forces) strongly depend on the partition of radiative energy into sensible and latent heat fluxes. This partition is determined to a large extent by the amount of water present in the top soil layers. As this variable is never measured routinely, the only way to address the problem is to simulate the soil water budget and the surface fluxes with the help of a model that can be integrated on a hourly basis over time scales of months or years.

This model must be simple, with as few parameters as possible. It must be able to accept standard meteorological data as inputs, and carry out a soil water budget. Such a model is presented here, along with some validation results. It is further shown, on an example, how it can be used to estimate the spread in sound levels (expressed here in terms of mean energy value L_{Aeq}) produced by long-term meteorological parameters, or the fraction of time during which a given sound pressure level is reached or exceeded, on a statistical basis.

2. THE SIMULATION MODEL

The model chosen is derived from the original model of Choisnel (1977), that was subsequently improved in many respects. It was primarily designed for agrometeorological purposes. The model simulates coupled energy and water transfer between the soil and the atmosphere. The vegetation is considered as a 'big-leaf' type surface layer. Convective fluxes (sensible and latent heat) are computed using the standard Monin-Obukhov similarity laws for turbulent transfer in the atmospheric boundary surface layer. Soil heat flux and temperature profiles are computed using the Fourier equation. A soil water balance is carried out at each time step, to estimate the amount of water that is available for the evaporation process.

The model is designed to be driven by standard meteorological data, and only requires a few easily available soil parameters. It runs on an hourly time step. The surface temperature T_s is computed by solving the energy budget equation. We first present the equations used for computing the surface fluxes. We then describe the water budget model and its coupling with surface processes.

2.1 Surface fluxes

2.1.1 The radiative budget

Net radiation R_n is computed as:

$$R_n = (1 - a)\, R_s + \varepsilon\, (R_a - \sigma\, T_s^4)$$

where R_s is the global radiation, R_a the atmospheric longwave radiation, T_s the radiative surface temperature and σ the Stefan-Boltzman constant.

R_s is estimated statistically from the daily sunshine fraction N (the ratio between the astronomical day length and the sunshine duration measured in meteorological networks). Computation of R_s first involves estimating the daily global radiation R_{sj} by an Angström type formula:

$$R_{sj} = R_{s0} (a_0 + b_0 N)$$

where R_{s0} is the extra-terrestrial radiation and a_0 and b_0 seasonal coefficients that depend on the location. Assuming that the fraction of diffuse solar radiation only depends on cloudiness, the daily diffuse radiation R_{dj} is computed in a similar way as:

$$R_{dj} = R_{s0} (a_1 + b_1 N)$$

The hourly values of direct ($R_i = R_s - R_d$) and diffuse (R_d) radiation are then estimated by weighting the daily values ($R_{sj} - R_{dj}$ and R_{dj}, respectively) by some function of solar elevation. This amounts to assuming that N is evenly distributed over the day. The hourly global radiation is finally estimated as $R_s = R_i + R_d$.

The atmospheric downward longwave radiation R_a is statistically estimated from the air temperature T_a and vapor pressure e_a:

$$R_a = \sigma [T_a - (33.5 - 18 \ln(e_a) + 1.7 e_a^{1/2}]^4 + 70 \text{ fneb}$$

with e_a expressed in mbar. The second term on the right hand side is a correction to account for the possible contribution of clouds. It involves the cloud fraction fneb, estimated from N through empirical relationships with coefficients depending on the season.

All the empirical coefficients used here have been established for oceanic climate in France (Choisnel, 1977).

The albedo a is computed using the model proposed by Baret et al. (1988), that simulates its hourly variation and accounts for the effect of surface characteristics on solar radiation absorption. It requires input parameters describing the vegetation structure (such as Leaf Area Index LAI, mean leaf inclination angle, optical properties of leaves and soil). Arbitrary values are assigned to the emissivity ε, according to the vegetation type.

2.1.2 Soil heat transfer

In the version of the model used here the soil is divided into four layers, with lower limits set at 10, 30, 50 and 100 cm, respectively. At the present stage only three main classes of soils (sand, loam, clay) are distinguished in the model (Table 1). The thermal characteristics are assumed to be homogeneous, with a uniform water content estimated from the available water stored (see further). The heat capacity c_s is computed by weighting linearly the heat capacity of each of the components (mineral, organic matter, air, water) by their

concentration (De Vries, 1963). The thermal conductivity λ_s is also determined from the type of soil and its mean water content (De Vries, 1963). For computing the soil temperature profile, the heat conservation equation and the Fourier law are solved in each soil layer:

$$\partial T / \partial t = - (1 / c_s) \partial G_z / \partial z \qquad \text{and} \qquad G_z = - \lambda_s \partial T / \partial z$$

G_z is the soil heat flux at depth z. The boundary conditions are given (1) at the bottom (z = 1 m) by a yearly sinusoidal variation of temperature, and (2) at the surface by a flux condition.

soil type	% mineral	wilting point	field capacity	s_u (mm/cm)
loamy	0.55	0.13	0.28	1.5
clay	0.50	0.27	0.45	2.2
sandy	0.55	0.05	0.15	1.0

Table 1. *Characteristics of the soil types (mineral matter content, water content at wilting point and field capacity, unit storage capacity in mm water by cm soil)*

Temperature T_1 computed at 10 cm is then used for estimating the ground heat flux G_0 at the surface by the Fourier equation. Following several authors (e.g., Shuttleworth and Wallace, 1985), we introduce a correction to account for the attenuation by the vegetation, assumed to be similar to the exponential attenuation of radiation under the vegetation layer:

$$G_0 = (\lambda_s / \Delta z) (T_s - T_1) \exp(-K\, LAI)$$

A value of 0.2 is assumed for the attenuation coefficient K.

2.1.3 Turbulent fluxes

Standard surface layer equations are used to compute sensible (H) and latent (LE) heat fluxes. H is given by:

$$H = \rho\, c_p (T_s - T_a) / r_a$$

where ρ and c_p are the air density and specific heat of air at constant pressure, respectively. T_a is the air temperature at height z, and r_a the aerodynamic resistance defined as:

$$r_a = \{ \ln[(z-d) / z_{0m}] - \Psi_m [(z-d) / L)] \} \{ \ln[(z-d) / z_{0h}] + \Psi_h [(z-d) / L] \} / k^2\, U$$

where U is the mean wind speed at height z and k the von Karman constant (k = 0.4). The parameters z_{0m} and d are the momentum roughness length and displacement height, respectively. They are estimated from crop height h_c using the common approximation $z_{0m} = 0.13\, h_c$ and $d = 0.66\, h_c$ (Brutsaert, 1982). The ratio z_{0h}/z_{0m} (z_{0h} being the thermal roughness length) may vary with the structure (density, height...) of the vegetation (Brutsaert, 1982). It can be prescribed in the model, but a value of 0.1 corresponding to a dense 'close' crop is often used. L is the Monin-Obukhov length defined as:

$$L = - \rho c_p T_a u_*^3 / k g H$$

where g is the acceleration due to gravity and u_* the friction velocity defined as:

$$u_* = k U \{ \ln[(z-d) / z_{0m}] - \Psi_m [(z-d) / L)] \}^{-1}$$

Ψ_m and Ψ_h are the common atmospheric stability functions, that can be found in Brutsaert (1982). A modification has been brought to the standard formulation that fails for very stable atmospheric conditions: an arbitrary threshold value of -5 has been set to avoid irrealistic values in this case.

The evapotranspiration at the soil-plant-atmosphere interface is estimated using the 'big-leaf' assumption (see Monteith, 1975):

$$LE = (\rho c_p / \gamma) [e_s(T_s) - e_a] / (r_a + r_*)$$

where γ is the psychrometric constant ($\gamma \approx 0.66$ hPa K^{-1}), e_a and $e_s(T_s)$ the air vapour pressure and the saturated vapour pressure at temperature T_s, respectively; r_* is the bulk surface resistance, computed following Katerji and Perrier (1985) who distinguish soil and canopy resistances in the following manner:

$$r_*^{-1} = (r_{0g} + r_g)^{-1} + (r_0 + r_s)^{-1}$$

r_{0g} is the resistance due to the vegetation structure. It is defined as (Katerji and Perrier 1985):

$$r_{0g} = 340 \text{ LAI}$$

r_g is the resistance of the soil layer to water transfer; it depends on the soil water content. It is a function of the ratio between the actual and maximum soil water availability. r_0 is a resistance to water vapor transfer through the canopy due to its structure; it varies from 5 to 10 s m^{-1} for meadow, from 10 to 20 s m^{-1} for wheat (Katerji and Perrier 1985). The stomatal resistance r_s is computed according to a model adapted from Noilhan and Planton (1989):

$$r_s = r_{s\,min} / (\text{LAI } F_1 F_2 F_3 F_4)$$

$r_{s\,min}$ is the minimum value of resistance in the absence of water stress (around 50 s m^{-1}). F_1, F_2, F_3 and F_4 are factors varying from 0 to 1, and are taken from Jacquemin and Noilhan (1990).

F_1 accounts for the influence of solar radiation and is parameterized after Dickinson (1984):

$$F_1 = (1 + f) / (f + r_{s\,min} / r_{s\,max})$$

with

$$f = (PAR / R_{s1}) (2 / \text{LAI})$$

$r_{s\,max}$ is the maximum crop stomatal resistance (set at 5000 $s\,m^{-1}$). PAR is the photosynthetically active solar radiation ($\approx 0.55\ R_s$). For the limit solar radiation R_{s1}, Noilhan and Planton (1989) propose a value of 100 $W\,m^{-2}$.

F_2 characterises the effect of soil water stress on stomatal regulation. It depends on the availability of water for extraction by the roots. It allows surface fluxes to depend on the soil water budget. Its parameterization is described in the next section.

F_3 accounts for the influence of air vapor pressure deficit (Jarvis, 1976):

$$F_3 = 1 - g_e\,(e_s(T_s) - e_a)$$

with $g_e = 0.025\ hPa^{-1}$ (Noilhan and Planton, 1989).

Finally, the effect of air temperature is introduced by the way of a F_4 factor (Dickinson, 1984):

$$F_4 = 1.0 - 0.0016\,(298 - T_a)^2$$

Finally, surface temperature and fluxes are simultaneously computed at each time step by solving the non-linear energy budget equation:

$$R_n\,(T_s) + G_0(T_s) + H(T_s) + LE(T_s) = 0$$

2.2 Soil water budget

Soil water transfer is simulated by a two-reservoir system (Jacquart and Choisnel, 1995). The maximum available amount of water R_{max} that can be extracted by the plants from the soil is defined as the difference between the soil water content at field capacity and at the wilting point. It may be prescribed from measurements, or estimated from soil maps (see Mori, 1982, for France). It depends on the thickness d_{max} of the cultivated soil layer and on the type of soil which characterizes the unit storage capacity s_u (see Table 1):

$$R_{max} = s_u\,d_{max}$$

The knowledge of s_u allows losses (evapotranspiration) and gains (rainfall, dew...) to be converted into an equivalent wetted soil thickness, which is then used for modifying the depths of the reservoirs at each time step.

The simulations are initialized at a date when the soil is saturated with water, in which case there is only one single reservoir (Figure 1a). The sequence of evaporation and rain phases lead to one- (Figure 1b) or two- (Figures 1c and 1d) reservoir systems, depending on the climatic conditions. At each time step rain is added on top of the soil. If the maximum available water limit is reached, excess rain is removed and converted into a runoff term - in the one-reservoir configuration -, or added to the lower part of the top reservoir - when there is one. In the latter case, the top reservoir may finally be filled up and a single-reservoir configuration is obtained again. Evaporated water is always extracted from the upper limit of

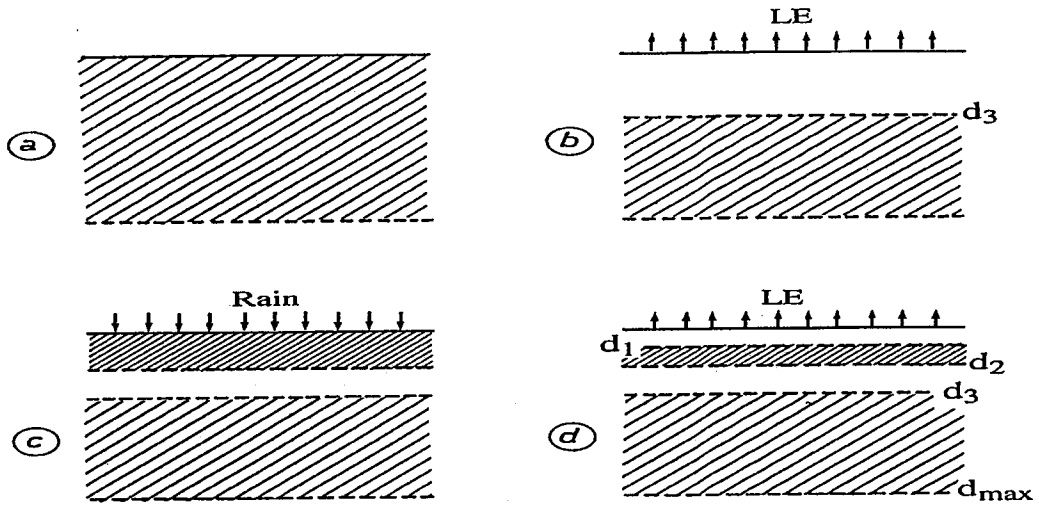

Figure 1. *Soil water budget model: an evaporation phase after initialisation (a) leads to a one-reservoir configuration (b). Sequences of rain and evaporation are simulated by a top reservoir (c, d).*

the top reservoir, until this surface reservoir completely dries out. Water is then extracted from the deep reservoir, which may dry out in turn, during long rain-free periods. The depths corresponding to the limits of the two reservoirs in the general case are d_1 and d_2 (top and bottom of the surface reservoir) and d_3 (top of the deep reservoir).

It has to be pointed out again that this model does not simulate a realistic water profile in the soil, but provides a good indicator of water availability at the surface. In particular the upper reservoir allows one to simulate events such as short periods of evaporation after rains occuring in dry conditions (summer rains for instance).

Defining d_4 as the depth of the reservoir nearest the surface ($d_4 = d_1$ or $d_4 = d_3$ in the one- and two-reservoir configurations respectively), the ratio d_4 / d_{max} is used for parameterizing the above mentioned F_2 factor that characterises the soil water stress: $F_2 = d_4 / d_{max}$.

The total amount of water in the soil at a given time is evaluated at each time step for computing the soil thermal characteristics. It corresponds to the sum of the water that cannot be extracted by evaporation (corresponding here to wilting point moisture), and of the remaining part of R_{max} that can be estimated as $R = s_u (d_{max} - d_3 + d_2 - d_1)$.

Two additional reservoirs have been introduced to account for dew (when evapotranspiration is negative) and interception of rain by vegetation. The amount of water I is accumulated in a reservoir (Calvet, 1990) whose maximum size I_x is defined by Dickinson (1984) as:

$$I_x = 0.2\ LAI$$

When it rains, this interception reservoir is filled first. If rainfall is greater than I_x, the excess water is distributed in the previous two soil reservoirs. As long as it exists, water is evaporated from the interception reservoir. Dew is accumulated in a fourth reservoir which is managed exactly as the interception reservoir. As long as intercepted rain or dew exist, a proportion d of surface covered by water is estimated following Noihlan and Planton (1989) as:

$$d = (I / I_x)^{2/3}$$

This factor appears in the computation of actual evapotranspiration LE, as a weighting term between potential evapotranspiration PET - corresponding to cases when the water remaining on leaf surfaces evaporates with no resistance - and the evapotranspiration of the canopy itself ET_c that is submitted to the stomatal regulation processes:

$$LE = d\ PET + (1 - d)\ Et_c$$

3. MODEL INPUTS AND OUTPUTS

3.1 Input meteorological data

Hourly air temperature T_a (h) and relative humidity Rh (h) are built from the minimum (T_{aN} and Rh_N, respectively) and maximum (T_{aX} and Rh_X, respectively) daily values using the following equations:

$$T_a (h) = T_{aN} + K_T(h) (T_{aX} - T_{aN})$$

$$Rh (h) = Rh_N + K_H(h) (Rh_X - Rh_N)$$

The coefficients $K_T(h)$ and $K_H(h)$ depend on the season and have been determined statistically. The hourly vapor pressure is then:

$$e_a = Rh (h)\ e_s(T_a)$$

In some cases, the only available information on air humidity is dew point temperature at 9:00 UT. The vapor pressure computed at this time is then considered as constant throughout the day.

As mentioned above, sunshine duration allows the hourly components of the solar radiation, and finally the net radiation, to be estimated. Windspeed is assumed to be constant all day long. This a rather strong assumption, and more realistic simulations would require time variations of this variable to be accounted for (particularly a day - night modulation). The daily rainfall is uniformly distributed over 24 hours.

3.2 Vegetation parameters

Mechanical and thermal roughness lengths are prescribed independently. The computation of the albedo with the model proposed by Baret et al. (1988) requires the type of

crop, the LAI and the mean leaf inclination angle to be prescribed. The emissivity value must also be known.

3.3 Soil parameters

The soil is assumed to be homogeneous. For the present time, three types of soil are defined in the model: loam, clay and sand. The soil composition, the thermal characteristics and the unit storage capacity s_u result from the choice of the soil type. Knowledge of the maximum available water amount is necessary. Soil minimum and maximun temperatures at 1 m, as well as the date of one of the extrema, are used to build the sinusoidal wave temperature required as a lower boundary condition for heat transfer computations.

3.4 Model outputs

The various surface fluxes and components of the radiative budget are computed every hour. The soil temperature profile and the soil water budget (configuration of the soil reservoirs, budget of the interception and dew reservoirs). The surface temperature is also an important output of the model. All these simulated data are synthetized for providing statistics (average values, extrema...) at daily and ten-day scales.

For the purpose of the present study the vertical gradients of mean horizontal wind speed and air temperature are calculated every hour from the standard Monin-Obukhov similarity laws:

$$\partial U / \partial z = [u_* / k (z_g - d)] \Phi_m [(z_g - d) / L]$$

$$\partial T / \partial z = [\theta_* / k (z_g - d)] \Phi_h [(z_g - d) / L]$$

where z_g is the desired height. The temperature scale θ_* is equal to $-H / (\rho c_p u_*)$ and the similarity functions are defined as:

$$\zeta \leq 0 \qquad \Phi_m^2 = \Phi_h = (1 - 16 \zeta)^{-1/2}$$
$$0 < \zeta < 1 \qquad \Phi_m = \Phi_h = 1 + 5 \zeta$$
$$1 < \zeta \qquad \Phi_m = \Phi_h = 6$$

In order to get the wind vector gradient, the mean wind speed gradient is projected onto the source - receiver direction.

4. MODEL VALIDATION

The model has not been extensively validated against a long-term dataset. Such data are missing at the present time, but will be available in the next future in the framework of the Alpilles/reSeDA experiment planned for 1997 in the South-East of France. Accordingly the model has been validated only for some outputs and for some experiments performed in particular climatic conditions.

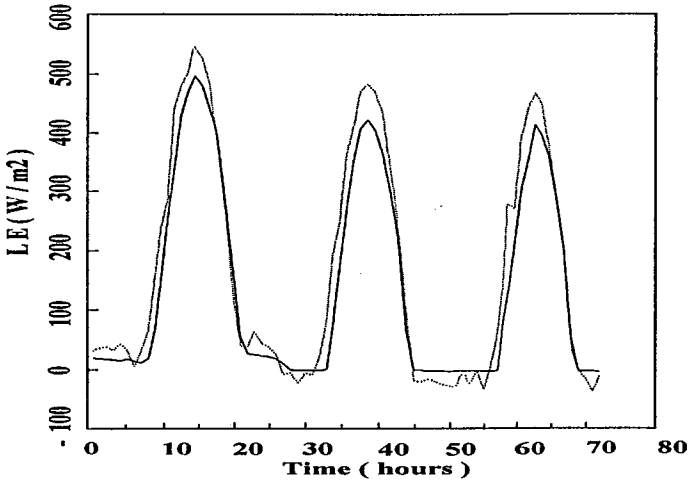

Figure 2. *Comparison between simulated (solid line) and measured (dotted line) latent heat flux over a soybean crop (Avignon, 18-20 August 1989).*

Figure 2 displays a comparison between actual evapotranspiration simulated with the model, and that measured over an irrigated soybean field, in Avignon. The overall agreement is satisfactory. It has to be pointed out that as the simulation is performed for maximum water availability, the coarse soil water budget model has not much effect here. For periods displaying both stressed and non-stressed conditions, we only present a comparison on surface temperatures (Figure 3). They have been recorded over a grass surface at Caumont airport (near Avignon) during an experiment performed over a seven month period (April to October 1986). Simulations have been performed using meteorological data recorded three kilometers away at an INRA station. The comparisons at the hourly scale (Figure 3a) and for

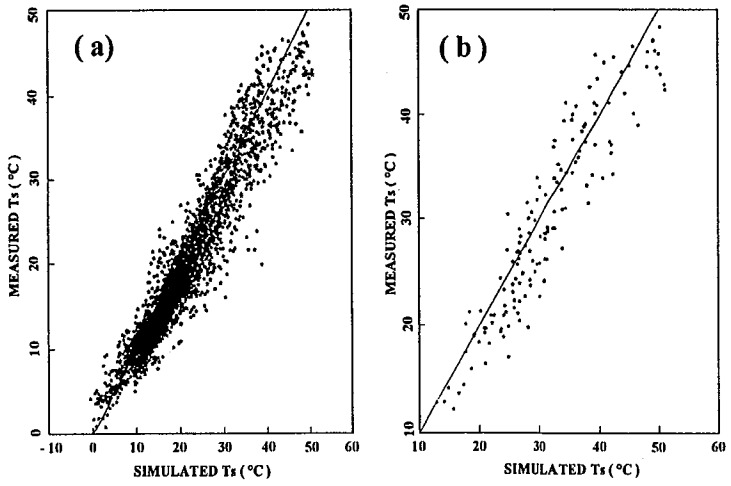

Figure 3. *Comparison between hourly (a) and maximum (b) simulated and measured surface temperature over a grass field (Avignon, April-October 1986)*

maximum daily temperatures (Figure 3b) are satisfactory. The scatter can primarily be related to the coarse assumption of a mean daily windspeed, and to possible discrepancies between simulated and actual soil water status which may induce differences at a few day scale. Nevertheless, we can think that the overall agreement observed in Figures 3a and 3b for surface temperature also implies a good agreement on surface fluxes.

The model was primarily designed for agrometeorological purposes and for long-term monitoring of surface water budget. The few previous examples of validation show that the simulated fluxes and surface temperatures agree rather well with the few available measurements. The model is not quite well suited for simulations at the hourly time scale for several reasons. First, the forcing variables are smoothed out because they are statistically re-built from daily meteorological data. Secondly the windspeed - that is responsible for large fluctuations in surface conditions and fluxes - is considered as constant, a rather severe assumption. Third, the coarse modelling of soil water budget makes it impossible to describe short time variations possibly related to rapid changes occuring in the top layers of soil. We must also mention that no coupling with a vegetation growth model exists at the present time: such a model would provide more realistic simulations throughout the year by introducing a link between the vegetation and the fluxes; as a matter of fact, plant development strongly depends on meteorological conditions (water status, drought for instance), and in return the plants determine the surface characteristics (structure, albedo, roughness...). Despite these limitations, the model seems realistic enough and appears as a good tool when only a statistical characterization of surface conditions over long periods is seeked.

5. AN ILLUSTRATIVE CASE STUDY

We used this model to estimate the micrometeorological parameters nedeed to compute long-range sound propagation. In this context the hourly determination of these factors allows the random fluctuations of this propagation to be taken into account. The principle of the methodology can be summarized as follows.

The chosen site is located in Angers, in the Loire valley (France). The necessary meteorological information was obtained from the standard meteorological network. In order to insure a statistically correct distribution, a 30 year period was selected. The climatic data was taken every 3 hours, in order to improve the representativity of the wind direction and velocity.

The climatic data set, along with local ground and vegetation parameters are used to feed the micrometeorological model. The latter enables us to obtain, at a given height and for given time intervals, the hourly values of the vertical air temperature and wind velocity gradients. Defining a particular source - receiver geometry, the wind vector gradient can then be computed, along with the vertical sound speed gradient and L_{Aeq} (using an appropriate acoustical model based on vertical sound gradients).

The calculations were performed for the particular case of a receiver located above a homogeneous flat grassy surface 320 m away from a point source. The heights of the receiver and the source are respectively 1.5 m and 6 m above the ground. The source is assumed to be located exactly to the North of the receiver.

As an example, Figure 4 shows the frequency distribution of the vertical sound speed gradient obtained at the mean height between the source and the receiver, i.e. z_g = 3.75 m.

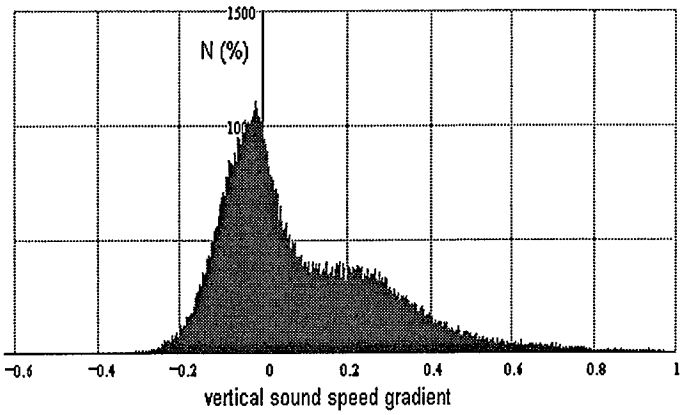

Figure 4. *Frequency distribution of the vertical sound speed gradient obtained at z_g = 3.75 m over the 30 year climatic series.*

In order to estimate L_{Aeq} (6 h - 22 h), we used the theoretical model described by Bérengier (1996) for positive sound speed gradients. For negative gradients, a set of experimental data were fitted to ensure a better accuracy in the shadow zone (Zouboff et al., 1994). Figure 5 shows the cumulative frequency distribution of L_{Aeq} (6 h - 22 h) over the 30 year period. As absolute values of L_{Aeq} depends on the power of the point source, the values given on the graph are not important per se.

This kind of chart can be very useful from a practical point of view: it allows one to

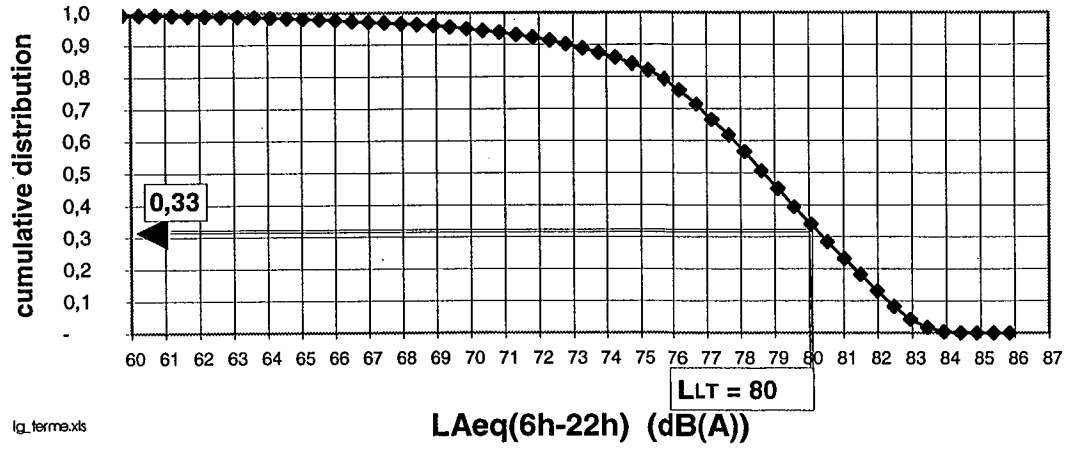

Figure 5. *Cumulative frequency distribution of L_{Aeq} (6 h - 22 h) obtained over the 30 year period, for the configuration described in the text.*

estimate the percentage of time during which a given acoustical value is reached or exceeded. For instance, using a practical method of calculation, we obtained a long-term L_{Aeq} level of 80 dB(A) for the same geometrical conditions as those described earlier. In Figure 5 it can be seen that this value can be reached or exceeded during about 33 % of the time.

6. CONCLUSION

The model presented here appears as a valuable tool for providing long-term statistical information on the microclimatic factors responsible for the propagation of sound in the lowest layers of the atmosphere. As the model was not primarily designed for this purpose, and as it was written about ten years ago, some improvements have to be made. In particular the parameterisation of the various resistances to the transfer of water has to be revised in the light of more recent studies. The treatment of heat and water transfer in the soil should also be improved. This is planned for the next future.

The model only allows the statistical properties of the sound pressure level to be estimated close to the meteorological measurements. In order to make this approach more general a methodology should be designed to provide a way of using the climatic data recorded by the meteorological network for estimating micrometeorological variables at locations not necessarily close to a particular station of this network. This is the subject of current research.

REFERENCES

Baret, F., Guyot, G., Teres, J.M., Rigal, D., 1988. Un modèle simplifié de réflectance et d'absorptance d'un couvert végétal. Proceedings of the 4th International colloquium on Spectral Signatures of Objects in Remote Sensing. ESA SP 287, Aussois,18-22 January 1988, 93-98.

Bérengier, M.C., 1996. Influence of propagating effects on the acoustical classification of road pavements. Internoise 96, Liverpool, 639-644.

Brutsaert, W.H., 1982. Evaporation into the atmosphere. Theory, history and applications. D. Reidel Publishing Company, London, England, pp. 299.

Calvet, J.C., 1990. Adaptation d'un modèle agrométéorologique au cas des couverts hétérogènes (vignes-vergers). DEA Astrophysique, Géophysique et Techniques Spatiales. Université Paul Sabatier et Ecole de la Météorologie, Toulouse, pp. 43.

Choisnel, E., 1977. Le bilan d'énergie et le bilan hydrique du sol. La Météorologie, numéro spécial Evapotranspiration, VI, 11, 103-133.

De Vries, D.A., 1963. Thermal properties of soils. In W.R. van Wijk (ed.) Physics of the Plant Environment, North Holland, Amsterdam, 210-235.

Dickinson, R.E., 1984. Modeling evapotranspiration from three-dimensional global climate models. In: Climate Processes and Climate Sensivity., Geophys. Monogr., 29, 58-72.

Jacquart, C., Choisnel, E., 1995. Un modèle de bilan hydrique simplifié à deux réservoirs utilisable en agrométéorologie. La Météorologie, 8, 29-43.

Jacquemin, B., Noilhan, J., 1990. Sensitivity study and validation of land surface parametrization using the Hapex-Mobilhy data set. Boundary Layer Meteorol., 52, 93-134.

Katerji, N., Perrier, A., 1985. Détermination de la résistance globale d'un couvert végétal à la diffusion de vapeur d'eau et de ses différentes composantes. Approche théorique et vérification expérimentale sur une culture de luzerne. Agric. For. Meteorol., 34, 105-120.

Monteith, J.L., 1975. Vegetation and the Atmosphere. Vol 1: Principles. Academic Press, New York, pp. 278.

Mori, A., 1982. Carte de France des réserves en eau des sols. Service d'Etude des Sols et de la Carte Pédologique de France, INRA, pp. 53 + 2 cartes.

Noilhan, J., Planton, S., 1989. A simple parametrization of land surface processes for meteorological models. Mon. Weather. Rev., 117, 536-549.

Shuttleworth, W.J., Wallace, J.S., 1985. Evaporation from sparce crops. An energy combination theory. Quart. J. Met. Soc., 111, 839-855.

Webb, E.K., 1970. Profile relationships: the log linear range and extension to strong stability. Quart. J. R. Met. Soc., 96, 67-90.

Zouboff, V., Brunet, Y., Bérengier, M., Séchet, E., 1994. A qualitative approach of atmospheric effects on long-range sound propagation. Sixth International Symposium on Long Range Sound Propagation, Ottawa, Canada, 12-14 June 1994, pp. 1 (summary).